JOURNAL OF GEOPHYSICAL RESEARCH, VOL. 103, NO. A7, PAGES 14,911-14,915, JULY 1, 1998

The latitude dependence of auroral roar

J. M. Hughes and J. LaBelle

Department of Physics and Astronomy, Dartmouth College, Hanover, New Hampshire

Abstract. LF/MF/HF radio receivers at many sites which extend from 66.5° to 79.9° invariant allow a statistical study of the variation of $2f_{ce}$ and $3f_{ce}$ auroral roar with latitude. At each of the sites, the frequency distribution is found to be approximately Gaussian, and the center frequencies of the distributions increase with the magnitude of the local geomagnetic field, as expected if the waves are associated with electron gyroharmonics. Furthermore, peak occurrence rates of $2f_{ce}$ auroral roar are found at 75°-76° invariant and show a strong correlation with Kp, including a 27-day periodicity. These data establish that auroral roar is associated with electron gyrofrequency harmonics and suggest that $2f_{ce}$ auroral roar originates near 275 km if it is generated at the second gyroharmonic.

1. Introduction

The auroral ionosphere is a prolific source of radio emissions, some of which are detectable on the ground. One such emission is auroral roar, which has a relatively narrow bandwidth ($\delta f/f \leq 0.1$) and occurs near 2 and 3 times the ionospheric electron gyrofrequency f_{ce}. Auroral roar near $2f_{ce}$ was first observed by *Kellogg and Monson* [1979], and $3f_{ce}$ roar was first reported by *Weatherwax et al.* [1993, 1995]. *LaBelle et al.* [1995] and *Shepherd et al.* [1998] present observations revealing the fine structure of $2f_{ce}$ roar and *Shepherd et al.* [1997], present data on the polarization. *Kellogg and Monson* [1984] report statistics of $2f_{ce}$ roar measured at Churchill, Manitoba, from 1979 to 1982. Despite this large quantity of previous work, it has not been established that the frequency of auroral roar varies with the magnitude of the geomagnetic field as expected if the emission is related to the electron gyrofrequency. In this brief report, we use data from multiple sites to investigate the latitude dependence of the occurrence rate and frequency of auroral roar.

2. Instrumentation

Dartmouth College has operated LF/MF/HF receivers in Alaska and at the south pole since 1991, at the Automated Geophysical Observatory P1 (AGO-P1) since 1994, and at the British Antarctic Survey (BAS-AGO) sites A80 and A81 since 1996. Also, since 1994, Dartmouth College has operated LF/MF/HF receivers at five sites in Canada: Gillam, Churchill, Arviat, Baker Lake, and Taloyoak, which extend from 66.8° to 79.2° invariant latitude along a geomagnetic meridian. Table 1 gives geographic coordinates and magnetic latitudes for these sites.

Data from the five Canadian sites are recorded with LF/MF/HF superheterodyne programmable receivers controlled by dedicated personal computers. These receivers sweep through 0.03-5.0 MHz every 2.0 s with 10-kHz resolution and operate 20 h/d, including all nighttime hours. Each of these systems uses a single-loop magnetic dipole antenna. A more detailed description of the instrumentation is given by *Weatherwax* [1994]. All data from these receivers are routinely displayed and archived as gray-scale survey spectrograms.

Figure 1 shows a typical survey spectrogram recorded at Baker Lake, Northwest Territories, on September 9, 1995. From 0200 to 0302 UT, a highly structured $2f_{ce}$ auroral roar event is visible from 2.7 to 3.1 MHz. Two other natural emissions, MF-burst and auroral hiss, are also visible in Figure 1: MF-burst is a broadband emission at 1.7-2.5 MHz during 0200-0204 UT and at 2.1-3.3 MHz during 0259-0302 UT, and auroral hiss is the emission below 530 kHz at 0257-0302 UT. The upper and lower frequency bounds of the auroral hiss are obscured by LF beacons and fixed-frequency AM transmitters which extend from approximately 30 kHz to 1.6 MHz and appear as horizontal lines in Figure 1. Because of ionospheric absorption, the amplitude of distant AM transmitters is generally higher during nighttime hours than during daytime hours. In this example, auroral substorm activity results in an abrupt absorption event which causes a sharp decrease in the amplitude of distant AM transmitters at 0200 UT. Despite the interference from the man-made transmissions, auroral roar emissions are easy to identify in the survey gray-scale plots, and their time duration and frequency range may be accurately measured by examining expanded plots.

Paper number 98JA01038.
0148-0227/98/98JA-01038$09.00

Table 1. Invariant Latitudes of Auroral Radio Receiver Sites

Site	Geographic Latitude	Geographic Longitude	Invariant Latitude
1 Gillam, Manit.	56.38	265.36	66.8
2 Churchill, Manit.	58.76	265.92	69.2
3 Arviat, NWT	61.11	265.95	71.4
4 Baker Lake, NWT	64.32	263.97	74.2
5 Taloyoak, NWT	69.54	266.45	79.2
6 Sondrestrom	66.99	309.05	73.3
7 Circle, Alaska	65.50	215.30	66.3
8 AGO-P1	-83.85	129.60	-79.9
9 BAS-AGO-A80	-81.50	3.00	-68.9
10 BAS-AGO-A81	-80.75	336.60	-66.5
11 South Pole	-90.00	N/A	-74.2

NWT, Northwest Terrirories; AGO, Automated Geophysical Observatory; BAS, British Antarctic Survey.

3. Data Presentation

3.1. Frequency Distribution

Weatherwax et al. [1995] obtained data on the frequency distribution of $2f_{ce}$ auroral roar events observed at Circle Hot Springs, Alaska, during October 1994 through June 1995. This distribution is approximately Gaussian with the center at 2825 kHz. The frequency distributions of $2f_{ce}$ auroral roar events observed at Churchill, Manitoba, for the years 1979 and 1982 were obtained by *Kellogg and Monson* [1984]. Again, the distributions are approximately Gaussian with the centers at 3030 and 3020 kHz, respectively.

These observations motivate compilation of the frequency distribution of $2f_{ce}$ auroral roar events at other sites. For each of the five Canadian sites and for the sites at Sondrestrom and AGO-P1, we used survey spectrograms of the type shown in Figure 1 to identify $2f_{ce}$ roar events and then made expanded plots which could be studied in detail. We then recorded the number of single-minute bins during which an event was observed in a given 10-kHz-wide bin. In this way, we obtained a frequency distribution for each site. A typical event has a bandwidth of 50-200 kHz, so that each single minute of auroral roar observation time contributes to several different frequency bins. Many hours of data from each of these sites were examined, including at least in 1-5 hours of $2f_{ce}$ auroral roar data at each site except the south pole, AGO-A80, and AGO-A81.

The distribution at each site was found to be approximately Gaussian, and the centroids were calculated. Using data from Table 1 and the National Space Science Data Center interface to the DGRF/IGRF geomagnetic field model, the magnetic field strength for each site was found as a function of altitude. Figure 2b shows the centroids of each frequency distribution plotted against the geomagnetic field strength at 275 km, the altitude for which previously analyzed $2f_{ce}$ auroral roar frequency distributions matched the electron gyroharmonic [*Weatherwax et al.*, 1995; *Kellogg and Monson*, 1984]. The error bars on each data point show the full width at half maximum of the Gaussian frequency distribution. Site identification numbers are located just above the horizontal axis and correspond to the numbers given in the first column of Table 1. There are three points marked with the number 2, identifying them with data that were recorded at Churchill during different years. Each of these points has a different field strength because of changes in the geomagnetic field over time.

A preliminary analysis has been performed on single $2f_{ce}$ auroral roar events observed at BAS-AGOs A80 and A81, and the frequency ranges of these two individual events are marked in Figure 2 with diamond symbols. The data from the south pole represent the

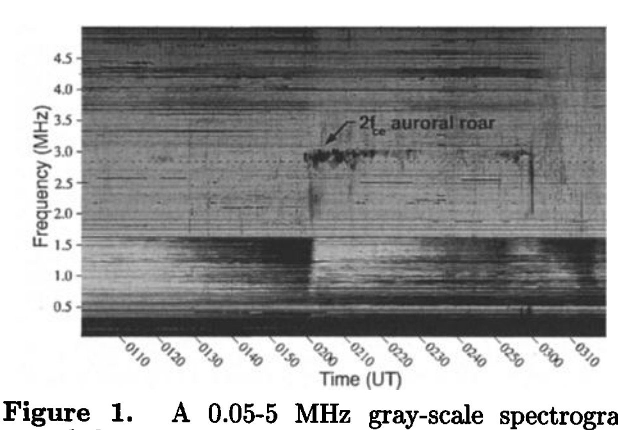

Figure 1. A 0.05-5 MHz gray-scale spectrogram recorded at Baker Lake, Northwest Territories, on September 9, 1995. From 0200 to 0302 UT, a $2f_{ce}$ auroral roar event occurs at 2.7-3.1 MHz.

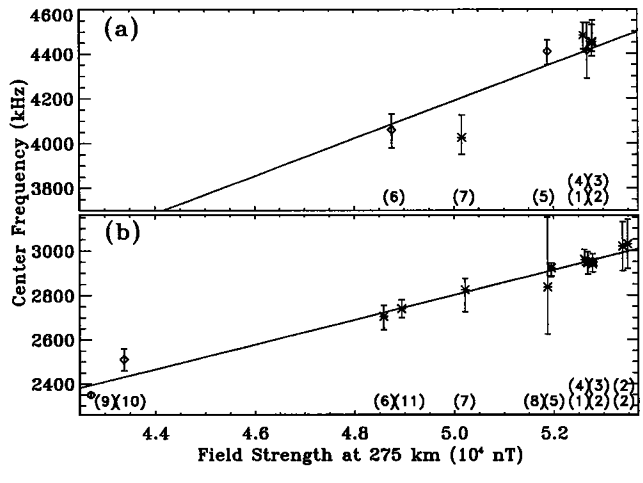

Figure 2. The centroids of the frequency distributions of $2f_{ce}$ and $3f_{ce}$ auroral roar at 11 sites plotted as a function of local ionsopheric magnetic field strength. The solid lines in Figures 2a and 2b show the slopes corresponding to $3f_{ce}$ and $2f_{ce}$, respectively, constrained to pass through the origin.

frequency range observed from three $2f_{ce}$ auroral roar events.

The center frequencies, both of the distributions and of the individual events, vary approximately linearly with magnetic field strength, as would be expected for emissions at frequencies related to harmonics of the electron gyrofrequency. A least squares fit to each of the data points is used to generate the fitted line shown in Figure 2b. This fitted line is required to pass through the origin and has a slope of 0.0560 kHz/nT and a linear correlation coefficient of 0.984. Considering the error bars in the individual measurements, the experimental error in this slope is approximately ±2%. Assuming that $2f_{ce}$ auroral roar does indeed occur at twice the electron gyrofrequency, the slope of the line in Figure 2 should be given by

$$\frac{d(2f_{ce})}{dB} = \frac{e}{\pi m_e} = 0.0560\,\mathrm{kHz/nT}$$

where e is the magnitude of the electron charge and m_e is the electron mass. The high linear correlation coefficient, showing that the center frequency of $2f_{ce}$ auroral roar varies linearly with the geomagnetic field strength, establishes that $2f_{ce}$ auroral roar is associated with electron gyrofrequency harmonics. Futhermore, if the source altitude is at 275 km as assumed in Figure 2, then $2f_{ce}$ auroral roar occurs within ±2% of the gyroharmonic. On the other hand, if a higher (lower) source altitude were assumed, the emission still varies linearly with f_{ce} but occurs at slightly above (below) $2f_{ce}$. For example, if the source altitude were 375 km, the slope implies emission at approximately $2.1f_{ce}$, ±2%.

The scenario for $3f_{ce}$ auroral roar is not as clear, partly because there are fewer observations of these emissions. Figure 2a shows observed frequency distributions of $3f_{ce}$ auroral roar emissions as a function of the geomagnetic field strength at 275 km. An analysis was performed similar to that described for Figure 2b, except that fewer stations were included. Data from Circle Hot Springs are taken from *Weatherwax et al.* [1995], and a few representative events are included from Taloyoak, Gillam, and Sondrestrom, represented by diamond symbols. The center frequency of $3f_{ce}$ roar increases with increasing magnetic field strength, as expected if the emissions are associated with electron gyroharmonics. However, the data are not sufficient to determine whether a linear relationship holds between frequency and magnetic field strength as for $2f_{ce}$ auroral roar. The solid line in Figure 2a is a least squares fit to the data points. This line has a slope corresponding to $3f_{ce}$ and is forced to pass through the origin. The 1994-1997 Canadian data appear consistent with generation at $3f_{ce}$ and 275 km, but the 1994-1995 Alaska data from *Weatherwax et al.* [1995] are not consistent with this line and would match $3f_{ce}$ only at a higher altitude of approximately 375 km. In summary, the existing data are not sufficient to draw firm conclusions about $3f_{ce}$ auroral roars; the center frequency increases with increasing magnetic field strength, but the relationship between center frequency and magnetic field strength may not be as simple as that found for $2f_{ce}$ roars.

3.2. Long-Term Variation of Occurrence Rate

Using survey spectrograms like the one shown in Figure 1, auroral roar events can be recognized and occurrence statistics determined. Figure 3a shows the auroral roar occurrence rate at Gillam, Churchill, and Arviat for a 6-month interval extending from September 18, 1994 to April 9, 1995. Every nighttime UT hour-interval during this 6-month period was investigated, and for each day, the nighttime hours containing $2f_{ce}$ auroral roar events were tallied. To obtain the occurrence rate, this number was then normalized by the total nighttime hours for which data were obtained. Figure 3a shows a 7-day running average of these values. Gaps in the data represent periods when no data were available.

Figure 3a shows that peaks in the occurrence rates are often separated by 27 days, the solar rotation period. However, in many cases, several peaks occur within a given 27-day interval. Autocorrelation analyses of each of these time series confirm spectral peaks corresponding to the 27-day period. The highest occurrence rates are observed during the spring equinoctial months when, on the most active nights, more than a third of the nighttime hours contain a $2f_{ce}$ auroral roar event. Figure 3a also shows that $2f_{ce}$ auroral roar events are less common at Gillam (66.8°) than they are at either Churchill (69.2°) or Arviat (71.4°), where occurrence rates are similar.

Figure 3b shows a 7-day running average of the global Kp index for the same 6-month period. There is a strong correlation between $2f_{ce}$ auroral roar occurrence

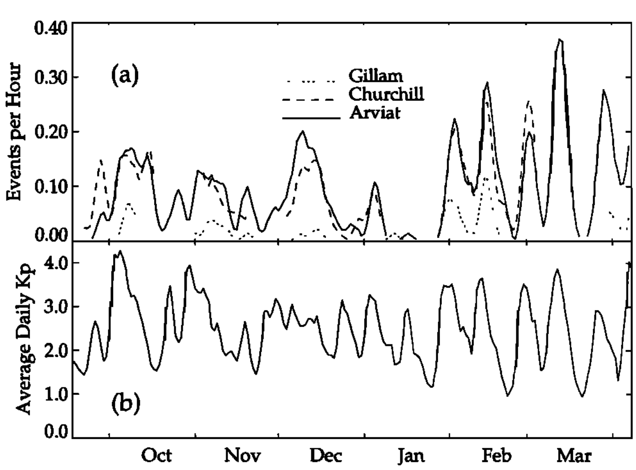

Figure 3. Occurrence rates of $2f_{ce}$ auroral roar events at three stations between September 1994, and April 1995. For comparison, a 7-day running average of the daily Kp for the same period is also shown.

rate and geomagnetic activity, represented here by K_p, with peaks in $2f_{ce}$ auroral roar occurrence rate corresponding to time periods of relatively high Kp, consistent with previous observations which show a close correlation between auroral roars and substorm onsets [*LaBelle et al.*, 1994].

Figure 3 shows, for some peaks, an approximately 1-day lag between peaks in K_p and the peak auroral roar occurrence rate. Cross-correlation analysis for these peaks confirms this 1-day lag. Figure 3 also shows that during this 6-month interval, the highest occurrence rates of the auroral roar emissions occur near equinox. This may reflect the Russell-McPherron effect, which results from the varying probability throughout the year of a southward component of the interplanetary magnetic field as seen by the magnetosphere and predicts maximum geomagnetic activity in early April and early October [*Russell and McPherron*, 1973].

3.3. Occurrence Rates

For the three sites studied in Figure 3a, the occurrence rate of $2f_{ce}$ auroral roar increases with invariant latitude. This result motivated us to investigate data from the higher-latitude Canadian sites at Baker Lake and Taloyoak. Two study-intervals were defined during which at least four out of the five Canadian sites were simultaneously operating. These intervals were September 25,1995 to November 5, 1995 and April 1,1997 to May 4,1997. During the first interval, data were analyzed from every day for which all five CANOPUS sites were active. Four of the CANOPUS sites were active on every day throughout the second interval, and data from each of these days were analyzed. For the days during the first interval which were analyzed, the daily average K_p index was 2.46, and during the second interval, the daily average K_p index was 1.97.

For each of the time periods analyzed, the auroral roar occurrence rate at each site was found by identifying the number of single-minute bins during which a $2f_{ce}$ auroral roar event was detected by the receiver system. The occurrence rate for each site is then found by normalizing the number of bins containing events by the total number of bins analyzed. For each site, 20 hours of data per day were analyzed, including all nighttime hours.

Figure 4 shows these occurrence rates as a function of invariant latitude. The dotted and dashed curves show the data from 1995 and 1997, respectively. The solid curve is a Gaussian fit $(Ae^{(x-x_0)^2/(2d^2)})$ to the 1995 data. The parameters determined by this least squares fit are $A = 0.054$, $x_0 = 75.36$, and $d = 4.07$. These results show that peak rates for the observation of $2f_{ce}$ auroral roar occur at approximately 75.4° invariant latitude and fall to half the peak rate at approximately 4.7° north or south of the peak latitude.

Consistent with the results drawn from Figure 3, the occurrence rates were higher for the selected 1995 interval than for the selected 1997 interval because of the previously mentioned difference in average geomagnetic activity during the two intervals. Although the 1995 and 1997 intervals show this expected difference in occurrence rates, both intervals indicate the same latitudinal dependence of $2f_{ce}$ auroral roar emissions. In both cases, Baker Lake is the most active, Gillam is the least active, and Taloyoak is more active than Churchill, implying that peak rates occur at an invariant latitude greater than that of Baker Lake. In both cases, the absolute occurrence rates shown in Figure 4 are lower than those determined by the methods of Figure 3a. This is due in part to the difference in the binning methods and to the inclusion of some daytime hours in the data of Figure 4.

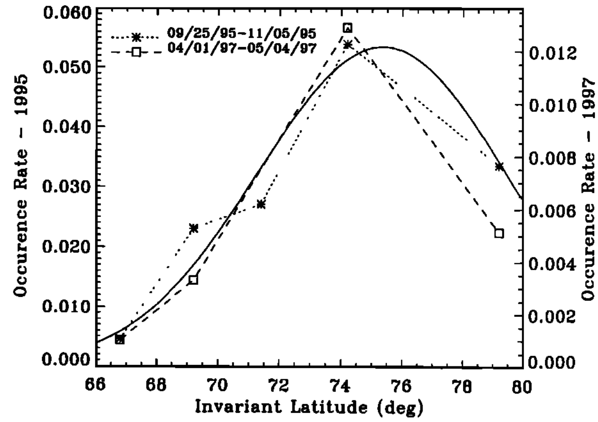

Figure 4. Occurrence rates of $2f_{ce}$ auroral roar at Canadian CANOPUS observatories as a function of invariant latitude.

In this discussion, it has been tacitly assumed that every roar that occurs is observed by ground-based instrumentation. However, it is quite possible that this assumption is not correct. Diffuse aurora can result in E layer critical frequencies above $2f_{ce}$ which would have the effect of screening our instrumentation from the auroral roar generation region [*Kellogg and Monson*, 1979]. Because of this screening, the rate at which auroral roars are observed at ground level would be lower than the rate at which they occur. Diffuse aurora occur near the equatorward edge of the auroral oval, which would extend from about 66° -72° invariant latitude at local magnetic midnight during times of moderate geomagnetic activity [*Kivelson and Russell (Eds.)*, 1995]. This screening may be one reason that ground-level occurrence rates are lower at the lower-latitude sites. For example, Gillam (66.8°) lies directly below regions of diffuse aurora, and therefore E region screening may be responsible for the low event rate there. Occurrence rates may peak in the ionospheric source region near the center of the nighttime auroral oval, and Figure 4 may represent the multiplication of this true occurrence rate with a filter function due to the E region screening.

Yoon et al. [1996] suggest that if an X mode maser process is responsible for the generation of $2f_{ce}$ auroral roar, the generation region might be associated with field-aligned auroral cavitites such as those investigated by *Doe et al.* [1993]. Other authors suggest Z mode mechanisms that also require such cavities [*Yoon et al.*, 1998; *Willes et al.*, 1998]. On the basis of radar data, *Doe et al.* [1993] show that auroral cavities lie just poleward of the statistical auroral oval and have an average invariant latitude of approximately 74.5°, which is very close to the peak latitude for the occurrence of auroral roar as determined from Figure 4 and almost directly above the site at Baker Lake, which registers the highest $2f_{ce}$ auroral roar occurrence rates.

4. Summary

Figure 2b shows that the center frequency of $2f_{ce}$ auroral roar varies linearly with the local geomagnetic field. If the source altitude is taken as 275 km, the slope of the line corresponds to emissions at $2.0f_{ce}$, within $\pm 2\%$. This result establishes that $2f_{ce}$ auroral roar is associated with electron gyrofrequency harmonics. The center frequency of $3f_{ce}$ auroral roar also increases with increasing geomagnetic field magnitude, as expected if these emissions are associated with the electron gyroharmonic. However, the data are not sufficient to indicate a linear relationship, though a least squares fit closely matches $3f_{ce}$ at 275 km.

Figure 3 shows that occurrence rates are strongly correlated with geomagnetic activity as measured with the K_p index. Figure 4 shows that in the Canadian sector, peak rates for the observation of $2f_{ce}$ auroral roar occur at nearly 75.4° invariant and fall to half the peak rate at latitudes approximately 4.7° north and south of the peak. This latitude of maximum ground-level activity may be shifted poleward of the real peak of $2f_{ce}$ auroral roar emissions at the source altitudes because of the effects of E region screening at auroral latitudes. Within the next several years, a larger data set will be available which will provide more certainty in these conclusions and may allow for the binning of occurrence rate statistics by quantities such as local time and K_p.

Acknowledgments. The research at Dartmouth College was supported by National Science Foundation grants ATM-9713119 and OPP-9615138. The authors thank Simon Shepherd for many helpful discussions, Mike Trimpi for his work on the Dartmouth receiver systems, and Barnaby Olson and Jane Parkin for their work, which contributed to Figures 2a and 3a. The authors also wish to thank British Antarctic Survey for support of receivers at AGOs A80 and A81, the CANOPUS contractors for support at CANOPUS observatories, the Canadian Geological Survey for support at Baker Lake, Antarcitic Support Associates for support at P1 and the south pole, SRI International for support at Sondrestrom, and Dawn Foster and Ron Drouin for support at Circle Hot Springs.

The Editor thanks Richard Horne and Allan Weatherwax for their assistance in evaluating this paper.

References

Doe, R. A., M. Mendillo, J. F. Vickrey, L. J. Zanetti, and R. W. Eastes, Observations of nightside auroral cavities, *J. Geophys. Res.*, *98*, 293, 1993.

Kellogg, P. J., and S. J. Monson, Radio emissions from the aurora, *Geophys. Res. Lett.*, *6*, 297, 1979.

Kellogg, P. J., and S. J. Monson, Further studies of auroral roar, *Radio Sci.*, *19*, 551, 1984.

Kivelson, M. G., and C. T. Russell (Eds.), *Introduction to Space Physics*, Cambridge Univ. Press, New York, 1995.

LaBelle, J., A. T. Weatherwax, M. L. Trimpi, R. Brittain, R. D. Hunsucker, and J. V. Olson, The spectrum of LF/MF/HF radio noise at ground level during substorms, *Geophys. Res. Lett.*, *21*, 2749, 1994.

LaBelle, J., M. L. Trimpi, R. Brittain, and A. T. Weatherwax, Fine structure of auroal roar emissions, *J. Geophys. Res.*, *100*, 21,953, 1995.

Russell, C. T., and R. L. McPherron, Semiannual variation of geomagnetic activity, *J. Geophys. Res.*, *78*, 92, 1973.

Shepherd, S. G., J. LaBelle, and M. L. Trimpi, The polarization of auroral radio emissions, *Geophys. Res. Lett.*, *24*, 3161, 1997.

Shepherd, S. G., J. LaBelle, and M. L. Trimpi, Further investigation of auroral roar fine structure, *J. Geophys. Res.*, *103*, 2219, 1998.

Weatherwax, A. T., Ground-based observations of auroral radio emissions, Ph.D. thesis, Dartmouth Coll., Hanover, N. H., 1994.

Weatherwax, A. T., J. LaBelle, M. L. Trimpi, and R. Brittain, Ground-based observations of radio emissions near $2f_{ce}$ and $3f_{ce}$ in the auroral zone, *Geophys. Res. Lett.*, *20*, 1447, 1993.

Weatherwax, A. T., J. LaBelle, M. L. Trimpi, R. A. Treumann, J. Minow, and C. Deehr, Statistical and case studies of radio emissions observed near $2f_{ce}$ and $3f_{ce}$ in the auroral zone, *J. Geophys. Res.*, *100*, 7745, 1995.

Willes, A. J., S. D. Bale, and Z. Kuncic, A *z* mode electron-cyclotron maser model for bottomside ionospheric harmonic radio emissions, *J. Geophys. Res.*, *103*, 7017, 1998.

Yoon, P. H., A. T. Weatherwax, T. J. Rosenberg, and J. LaBelle, Lower ionospheric cyclotron maser theory: A possible source of $2f_{ce}$ and $3f_{ce}$ auroral radio emissions, *J. Geophys. Res.*, *101*, 27,015, 1996.

Yoon, P. H., A. T. Weatherwax, and T. J. Rosenberg, On the generation of auroral radio emissions at harmonics of the lower ionospheric electron cyclotron frequency: X, O, and Z mode maser calculations, *J. Geophys. Res.*, *103*, 4071, 1998.

J. M. Hughes and J. LaBelle, Department of Physics and Astronomy, Dartmouth College, Hanover, NH 03755. (e-mail: hughesj@coos.dartmouth.edu; jlabelle@einstein.dartmouth.edu)

(Received December 1, 1997; revised March 10, 1998; accepted March 25, 1998.)